Interplay of Phenol and Isopropyl Isomerism in Propofol from Broadband Chirped-Pulse Microwave Spectroscopy

ARTICLE *in* JOURNAL OF THE AMERICAN CHEMICAL SOCIETY · SEPTEMBER 2010

Impact Factor: 12.11 · DOI: 10.1021/ja104950w · Source: PubMed

J|A|C|S
ARTICLES

Published on Web 09/07/2010

Interplay of Phenol and Isopropyl Isomerism in Propofol from Broadband Chirped-Pulse Microwave Spectroscopy

Alberto Lesarri,*,† Steven T. Shipman,‡,1 Justin L. Neill,‡ Gordon G. Brown,‡,2 Richard D. Suenram,‡ Lu Kang,§ Walther Caminati,|| and Brooks H. Pate*,‡

Departamento de Química Física y Química Inorgánica, Facultad de Ciencias, Universidad de Valladolid, 47011 Valladolid, Spain, Department of Chemistry, University of Virginia, McCormick Road, Charlottesville, Virginia 22904, Department of Chemistry, Southern Polytechnic State University, 1100 South Marietta Parkway, Marietta, Georgia 30060, and Dipartimento di Chimica "G. Ciamician", Università di Bologna, Via Selmi 2, 40126 Bologna, Italy

Received June 7, 2010; E-mail: lesarri@qf.uva.es; brookspate@virginia.edu

Abstract: The conformational equilibrium of the general anesthetic propofol (2,6-diisopropylphenol) has been studied in a supersonic expansion using broadband chirped-pulse microwave spectroscopy. Three conformers originated by the combined internal rotation of the hydroxyl and the two isopropyl groups have been detected in the jet-cooled rotational spectrum. The most stable conformer exhibits tunneling splittings associated with the internal rotation of the hydroxyl group, from which we determined the torsional potential and barrier heights (905−940 cm^{-1}). The carbon backbone structure was derived from the spectral assignments of all 12 ^{13}C monosubtituted isotopologues in natural abundance and confirmed a plane-symmetric gauche orientation of the two isopropyl groups (Gg) for this conformer. In the other two detected conformers (EG and GE) one of the isopropyl groups is eclipsed with respect to the ring plane while the other is gauche, differing in a ∼180° rotation of the hydroxyl group. Supporting ab initio calculations provided information on the potential energy surface and molecular properties of the title compound.

Introduction

The molecular mechanisms of anesthetic action have been elusive for years. Currently it is commonly admitted that anesthetics operate by directly binding to protein targets, i.e., neuronal ligand-gate ion channels, but the identity of the protein receptors and binding sites is still uncertain in most cases. There are a few high-resolution (2−3 Å) crystal structures of anesthetics bound to soluble proteins obtained by X-ray diffraction,[1−3] but to date, it has not been possible to obtain crystal structures of integral membrane proteins. In consequence, most information on anesthetic functions comes from solution or computational studies.

Alternatively, gas-phase experiments are emerging as an important source of structural data for molecules of biological interest.[4−6] Gas-phase investigation of anesthetics and their weakly bound clusters can be used to model conformational landscapes and local interactions with large macromolecular receptors, reducing the complexity of native biostructures and gaining information on specific noncovalent interactions at the active site. Gas-phase studies additionally benefit from a direct comparison to in vacuo theoretical predictions.

Multiple characterization methods, mostly high-resolution spectroscopic techniques, have been exploited to derive structural and conformational information of gaseous systems, but these have been applied typically to relatively small molecules.[4−6] In particular, spectroscopy in the microwave region has been the method of choice for determination of gas-phase structures but is usually limited to molecules of 10−20 atoms and few degrees of freedom. Expanding the capabilities of microwave spectroscopy to larger systems requires a different approach to conventional spectrometers in order to suppress their traditional frequency and bandwidth constraints. The recent introduction of chirped-pulse Fourier transform microwave (CP-FTMW) spectroscopy[7−10] is a major step forward in this direction. Presently, bandwidth capabilities in the cm-wave region have been expanded 4 orders of magnitude with respect to conven-

† Universidad de Valladolid.
‡ University of Virginia.
[1] Current address: Division of Natural Sciences, New College of Florida, 5800 Bay Shore Road, Sarasota, Florida 34243.
[2] Current address: Department of Chemistry, Coker College, 300 East College Avenue, Hartsville, South Carolina 29550.
§ Southern Polytechnic State University.
|| Università di Bologna.

(1) (a) Bhattacharya, A. A.; Curry, S.; Franks, N. P. *J. Biol. Chem.* **2000**, *275*, 38731. (b) Vedula, L. S.; Brannigan, G.; Economou, N. J.; Xi, J.; Hall, M. A.; Liu, R.; Rossi, M. J.; Dailey, W. P.; Grasty, K. C.; Klein, M. L.; Eckenhoff, R. G.; Loll, P. J. *J. Biol. Chem.* **2009**, *284*, 24176.
(2) Franks, N. P.; Jenkins, A.; Conti, E.; Lieb, W. R.; Brick, P. *Biophys. J.* **1998**, *75*, 2205.
(3) Verschueren, K. H. G.; Seljée, F.; Rozeboom, H. J.; Kalk, K. H.; Dijkstra, B. W. *Nature* **1993**, *363*, 693.
(4) Schermann, J. P. *Spectroscopy and Modeling of Biomolecular Building Blocks*; Elsevier: Amsterdam, 2008.
(5) de Vries, M. S.; Hobza, P. *Annu. Rev. Phys. Chem.* **2007**, *58*, 585.
(6) (a) Weinkauf, R.; Schermann, J.-P.; De Vries, M. S.; Kleinermanns, K. *Eur. Phys. J. D* **2002**, *20*, 309. (b) Robertson, E. G.; Simons, J. P. *Phys. Chem. Chem. Phys.* **2001**, *3*, 1.

tional Balle−Flygare[11] FTMW spectrometers and its operation has been extended down to 2 GHz.[12]

In this work, we used chirped-pulse microwave spectroscopy to investigate the ground-state structural properties of propofol (2,6-diisopropylphenol). Propofol is a common alkylphenol short-acting general anesthetic introduced in clinical practice in the 1980s. As in other general anesthetics, the molecular mechanisms of action are believed to target the γ-aminobutyric acid type A ($GABA_A$) receptors,[13] but present information is limited to complexes with proteins not involved in anesthetic action[1] and computational studies.[14,15] This work is thus intended to be a first step in the investigation of the molecular properties and intermolecular clusters of the title compound. Propofol is also an interesting case of multiple rotational isomerism because of the presence of two isopropyl chains and a hydroxyl group, in which the symmetry of the lateral chains allows for (in certain conformers) a quantitative evaluation of the large amplitude motion of the hydroxyl group. At the same time, this 31-atom molecular system serves as a test of the capabilities and sensitivity of the CP-FTMW spectrometer. No previous high-resolution spectroscopic studies of propofol were available, making this work also valuable to assess the theoretical methods used in computer modeling of this anesthetic.

Experimental and Theoretical Methods

The jet-cooled rotational spectrum of propofol was studied with a CP-FTMW spectrometer developed at the University of Virginia. Chirped-pulse spectrometers produce ultrabroadband (11 GHz) fast-passage[16,17] excitation in the microwave region, resulting in a transient spontaneous emission between rotational levels that can be collected in the time-domain. Subsequent spectral analysis using a Fourier transform yields the resonance frequencies of the rotational transitions. The chirped-pulse methods have been reviewed recently,[7−10,12,18] so only brief details relevant to this experiment are necessary here.

The microwave source was a 24 GS/s arbitrary waveform generator, producing a 12−0.5 GHz linear frequency sweep in 1 μs. This pulse was upconverted in a triple-balanced mixer by an 18.95 GHz phase-locked resonant dielectric oscillator (PLDRO), probing the entire 7−18.5 GHz frequency range in a single event. Power amplification of the chirped pulses was performed with a pulsed 300 W traveling-wave-tube amplifier. The amplified pulse interacts with the pulsed supersonic jet in a high-vacuum chamber, using two standard-gain microwave horns to transmit and receive the microwave radiation. The receiver is protected from the high-power pulse by a passive PIN diode limiter and a single-pole single-throw microwave switch. The resulting microwave free-induction-decay (FID) was amplified and digitized directly on a 50 GS/s oscilloscope with 16 GHz of hardware bandwidth. As discussed in ref 9, multiple microwave excitation/detection sequences can be applied on each valve injection, reducing sample consumption. For this experiment, 10 pulses were applied on each of 60 000 valve injection cycles for a total of 600 000 rotational FIDs averaged for the final spectrum. The phase reproducibility of the experiment is achieved by locking all frequency sources and the digital oscilloscope to a 10 MHz Rb-disciplined quartz oscillator. Each FID was acquired for 20 μs. The nozzle was run at a repetition rate of 0.6 Hz, limited by the data processing speed of the digital oscilloscope. The total measurement time was 28 h.

The sample of propofol (97%) was obtained commercially and used without any further purification. Propofol is a liquid with a low melting point (mp 18 °C, vapor pressure of 5.6 mmHg at 100 °C), so in order to create a gas-phase sample, it was placed in a nozzle (general valve, 0.9 mm diameter) modified to accommodate a sample reservoir and fitted with a resistive heater.[19] Optimal signal levels were observed at temperatures of approximately 100 °C. A mixture of approximately 80% neon and 20% helium with a backing pressure of ~150 kPa was flowed over the sample before expansion into the vacuum chamber.

The investigation of the rotational spectrum was supplemented with ab initio electronic structure calculations. Different theoretical methods and basis sets were used during the course of this work, as implemented in the Gaussian 03 suite of programs.[20] Initially DFT theory and Becke's B3LYP hybrid functional were used to complete a relaxed two-dimensional scan of the potential energy surface (PES), using the torsion angles of the two isopropyl groups (as defined in Figure 1) as independent variables. Results are shown in Figure 2 for the triple-ζ 6-311++G(d,p) basis set. Additionally, the structures of the stable conformers of propofol were reoptimized using MP2-FC and the 6-311++G(d,p) and cc-pVTZ basis sets. Harmonic frequency calculations confirmed that the predicted conformers are true minima at this level of theory.

Results

Potential Energy Surface. The PES presented in Figure 2 shows that several competing conformers originated by the torsion of the hydroxyl and the two isopropyl groups contribute to the conformational landscape of propofol. The four wells in Figure 2 are separated by relatively high barriers (>1000 cm^{-1}), so conformational relaxation[21] between these basins in the supersonic expansion is likely to be negligible, and multiple conformers could be simultaneously populated in the jet-cooled expansion.

The lowest-lying well accommodates two distinct conformers adopting a gauche (G) arrangement of the isopropyl α-hydrogen with respect to the phenyl ring. These two conformers were denoted GG and Gg depending on whether the two isopropyl groups are rotated conrotatory (GG) or disrotatory (Gg) with respect to the ring. DFT-B3LYP predicts GG to be the global minimum but with the Gg structure only 29 cm^{-1} above GG

(7) Brown, G. G.; Dian, B. C.; Douglass, K. O.; Geyer, S. M.; Pate, B. H. *J. Mol. Spectrosc.* **2006**, *238*, 200.
(8) Shipman, S. T. Pate, B. H. Broadband Fourier Transform Microwave Spectroscopy. In *Handbook of High-Resolution Spectroscopy*; Quack, M., Merkt, F., Eds.; Wiley-VCH: Weinheim, Germany, 2010.
(9) Brown, G. G.; Dian, B. C.; Douglass, K. O.; Geyer, S. M.; Shipman, S. T.; Pate, B. H. *Rev. Sci. Instrum.* **2008**, *79*, 53103.
(10) Dian, B. C.; Brown, G. G.; Douglass, K. O.; Pate, B. H. *Science* **2008**, *320*, 994.
(11) Balle, T. J.; Flygare, W. H. *Rev. Sci. Instrum.* **1981**, *52*, 32.
(12) Shipman, S. T.; Alvarez-Valtierra, L.; Neill, J. L.; Pate, B. H.; Lesarri, A.; Kisiel, Z. Presented at the 63rd International Symposium on Molecular Spectroscopy, Columbus, OH, June 16−20, 2008; WF08.
(13) (a) Trapani, G.; Altomare, C.; Sanna, E.; Biggio, G.; Liso, G. *Curr. Med. Chem.* **2000**, *7*, 249. (b) Krasowski, M. D.; Nishikawa, K.; Nikolaeva, N.; Lin, A.; Harrison, N. L. *Neuropharmacology* **2001**, *41*, 952. (c) Bali, M.; Akabas, M. H. *Mol. Pharm.* **2004**, *65*, 68.
(14) Bertaccini, E. J.; Trudell, J. R.; Franks, N. P. *Anesth. Analg.* **2007**, *104*, 318.
(15) Campagna-Slater, V.; Weaver, D. F. *Neurosci. Lett.* **2007**, *418*, 28.
(16) McGurk, J. C.; Schmalz, T. G.; Flygare, W. H. *J. Chem. Phys.* **1974**, *60*, 4181.
(17) Schmalz, T. G.; Flygare, W. H. Coherent Transient Microwave Spectroscopy and Fourier Transform Methods. In *Laser and Coherence Spectroscopy*; Steinfeld, J. I., Ed.; Plenum Press: New York, 1978; pp 125−196.
(18) Grabow, J.-U.; Caminati, W. Microwave Spectroscopy: Experimental Techniques. In *Frontiers of Molecular Spectroscopy*; Elsevier: Amsterdam, 2008; Chapter 14.
(19) Suenram, R. D.; Lovas, F. J.; Plusquellic, D. F.; Lesarri, A.; Kawashima, Y.; Jensen, J. O.; Samuels, A. C. *J. Mol. Spectrosc.* **2002**, *211*, 110.
(20) Frisch, M. J.; et al. *Gaussian 03*; Gaussian, Inc.: Wallingford, CT, 2004.
(21) (a) Ruoff, R. S.; Klots, T. D.; Emilsson, T.; Gutowsky, H. S. *J. Chem. Phys.* **1990**, *93*, 3142. (b) Godfrey, P. D.; Brown, R. D. *J. Am. Chem. Soc.* **1998**, *120*, 10724.

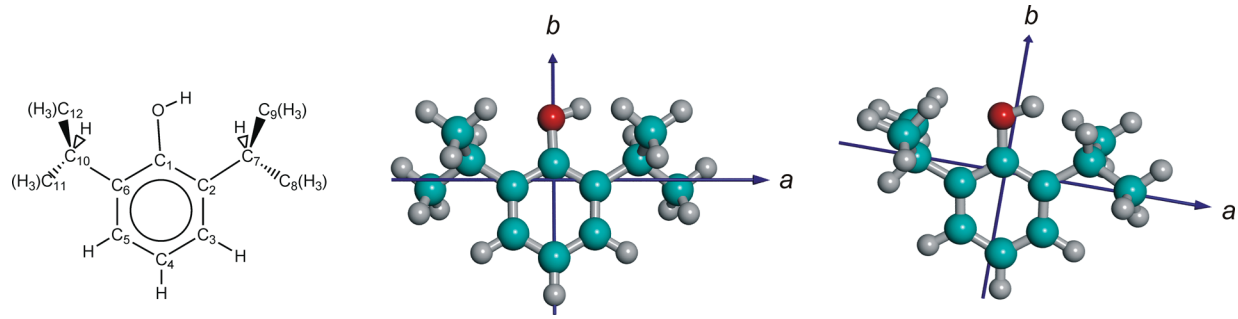

Figure 1. Atom labeling and orientation of the principal inertial axes in conformers Gg (most stable structure, left) and EG (right) of propofol. The dihedral angles for the isopropyl torsions were defined as $\tau_1 = (H{-}C_{10}{-}C_6{-}C_1)$ and $\tau_2 = (H{-}C_7{-}C_2{-}C_1)$.

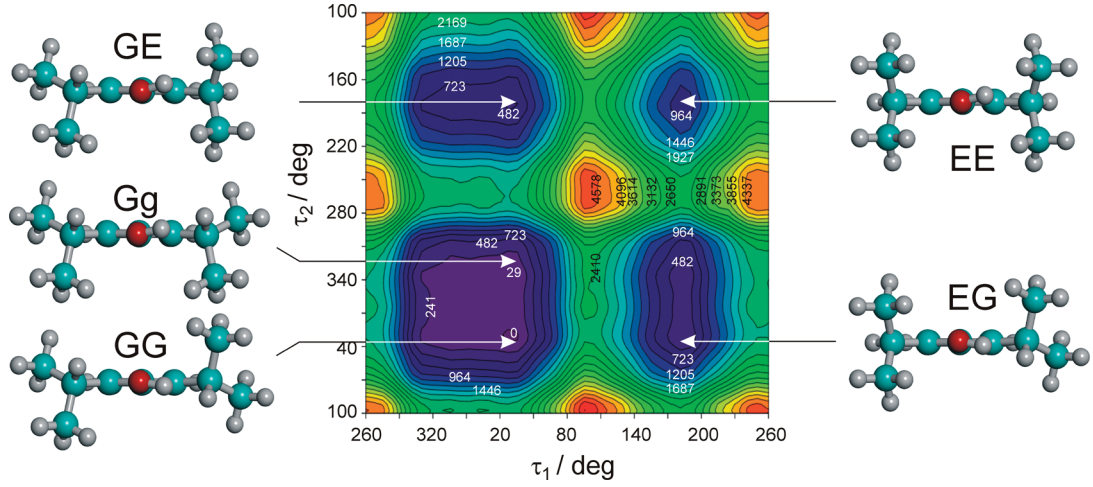

Figure 2. The DFT (B3LYP/6-311++G(d,p), cm^{-1}) potential energy surface of propofol shows four wells and five distinct local minima. The two most stable structures exhibit gauche orientations of the isopropyl groups, either on the same side (Gg) or on different sides (GG) of the phenyl ring. Eclipsing one or two of the isopropyl groups produces the three higher energy minima. The independent variables correspond to the torsion angles τ_1 and τ_2 defined in Figure 1.

Table 1. Ab Initio Rotational Parameters of Propofol Using MP2/6-311++G(d,p)

parameter[a]	conformer Gg	conformer GG	conformer EG	conformer GE	conformer EE
A/MHz	1464.3	1466.6	1327.1	1325.5	1171.3
B/MHz	509.4	499.7	540.0	537.4	589.5
C/MHz	421.8	424.8	446.5	445.2	473.4
P_{cc}/u Å^2	69.56	83.13	92.40	93.19	110.54
Δ_J/kHz	0.013	0.009	0.012	0.013	0.013
Δ_{JK}/kHz	−0.005	0.037	0.004	0.009	0.009
Δ_K/kHz	0.055	0.013	0.037	0.034	0.014
δ_J/kHz	0.004	0.002	0.003	0.003	0.003
δ_K/kHz	0.058	−0.030	−0.021	−0.039	−0.081
μ_a/D	1.58	1.57	1.66	1.68	1.77
μ_b/D	−0.27	−0.32	−0.39	0.01	−0.13
μ_c/D	0.29	−0.22	−0.26	0.35	0.33
μ_{total}/D	1.63	1.62	1.72	1.71	1.80
E/E_h	−541.85848	−541.85854	−541.85795	−541.85640	−541.85559
E + ZPE[b]/E_h	−541.58374	−541.58386	−541.58343	−541.58201	−541.58142
ΔE/cm^{-1}	14.0	0.0	130.6	470.4	647.1
$\Delta(E + ZPE)$/cm^{-1}	25.9	0.0	93.9	405.8	536.0

[a] Rotational constants (A, B, C), planar moment ($P_{cc} = (1/2)(I_a + I_b - I_c) = \sum_i m_i c_i^2$), Watson's A-reduced centrifugal distortion constants (Δ_J, Δ_{JK}, Δ_K, δ_J, δ_K) and electric dipole moment components (μ_α, $\alpha = a, b, c$). [b] Zero-point energy correction.

and a very low isomerization barrier (Figure S1 in Supporting Information). In the next two wells one of the isopropyl groups adopts a gauche arrangement while the other is eclipsed (E) by the ring. These conformers are denoted EG (hydroxyl proton on the gauche isopropyl side) and GE (hydroxyl proton on the eclipsed isopropyl side), differing only by a ∼180° internal rotation of the hydroxyl group. The highest energy well corresponds to a single minimum (EE), with the two isopropyl groups eclipsed by the ring. The calculated rotational parameters for the five local minima reoptimized with MP2-FC are presented in Tables 1 (6-311++G(d,p)) and S1 (cc-pVTZ, Supporting Information).

Rotational Spectrum of Propofol Gg. The CP-FTMW spectrum of propofol is presented in Figure 3. Guided by the ab initio calculations presented above, a rotational spectrum was assigned that accounted for the strongest lines in the spectrum.

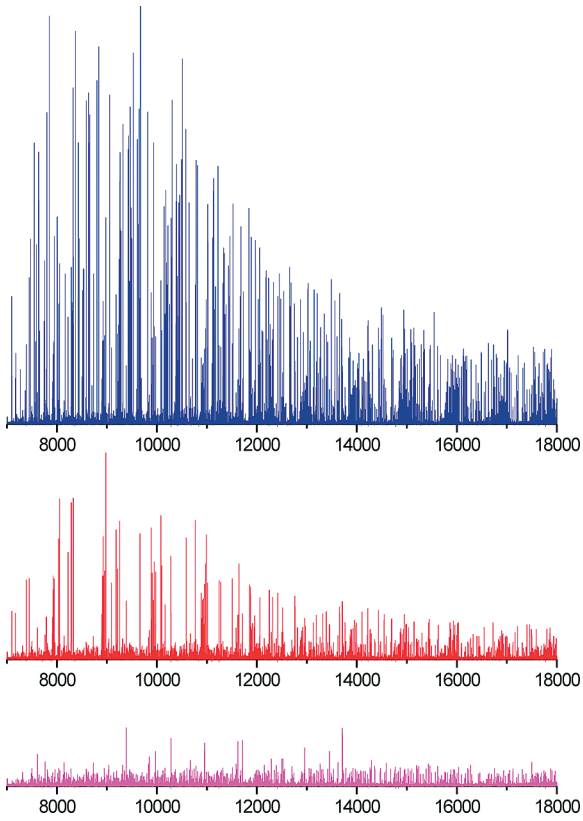

Figure 3. Microwave spectrum of propofol in the frequency range 7−18 GHz (upper blue trace), obtained with a chirped-pulse FTMW spectrometer after 600 000 averaging cycles. The full 11 GHz bandwidth spectrum is acquired on each measurement cycle. The spectrum is dominated by transitions from propofol Gg. The center trace shows the spectrum after subtraction of conformer Gg, which led to the assignment of conformer EG. The weaker signals from conformer GE and all ^{13}C species of conformer Gg were later detected after subtraction of the spectra of conformers Gg and EG (lowest trace).

The analysis of the full-bandwidth rotational data was assisted by Plusquellic's JB95 program suite, allowing for graphical simulation and fitting.[22] Transitions with *a*-, *b*-, and *c*-type selection rules were found, with intensities indicating $\mu_a > \mu_b > \mu_c$. As illustrated in Figure 4, all *a*-type transitions were split into two components separated by approximately 208.2 MHz, nearly independent of the rotational quantum numbers (Table S2), while the weaker *b*- and *c*-type transitions were unsplit. Similar tunneling splittings have been observed in phenol[23] and its symmetric para-derivatives.[24,25] In phenol, transitions with *b*-type selection rules are split. However, in propofol the two bulky isopropyl groups cause the *a* and *b* principal inertial axes to exchange, so the μ_a splittings of this propofol conformer correspond to the μ_b doublets of other symmetric phenols. This frequency doubling is due to internal rotation of the hydroxyl group, splitting the ground vibrational state ($v = 0$) into two torsional sublevels ($\sigma = 0, 1$). The fact that the internal rotation inverts the sign of μ_a suggests that the split lines are the two interstate transitions ($\sigma = 1 \leftarrow 0$ or $0 \leftarrow 1$) of the OH internal rotation. The rotational transitions were analyzed with a two-state Hamiltonian without coupling terms, i.e.,

$$\begin{pmatrix} H_0 & 0 \\ 0 & H_1 + \Delta E_{10} \end{pmatrix} \quad (1)$$

where H_0 and H_1 are semirigid-rotor Hamiltonians and ΔE_{10} is the relative energy between the two torsional substates.

The results of global two-state fits[26] using a Watson's A-reduction semirigid rotor Hamiltonian[27,28] (I^r representation) for a set of 575 observed transitions (Tables S3−S6) are presented in Table 2. In fit 1, the rotational and quartic distortion constants of the two torsional substates were fit independently, while in fit 2 they were constrained to the same values. While Coriolis interactions between the two substates were neglected, we considered that these contributions might be appreciable in cases where the asymmetry and torsional splitting were accidentally close. However, we observed only a few slight deviations (~100 kHz) from the semirigid behavior, which were not included in the final fit. No evidence was found for tunneling effects associated with the internal rotation of the methyl groups, as in similar molecules.[29]

The identification of the structure associated with this spectrum could not rely only on the ab initio predictions of the rotational constants and relative dipole moment components, since the two lowest-lying conformers (GG and Gg) have similar rotational constants and are calculated to be very close in energy. In order to provide an unequivocal conformational assignment, we assigned the spectra of all 12 ^{13}C-monosubstituted species in natural abundance (1.1%, Figure S2). Assignment of the spectrum of the ^{18}O species was not attempted because of its lower natural abundance (0.2%). In the analysis of the ^{13}C species we noticed that a single isotopic substitution in any position off the axis for the OH internal rotation (i.e., all carbon atoms except C_1 and C_4 in Figure 1) breaks down the equivalence between the two isopropyl groups, annihilating the tunneling splitting. For the two isotopologues exhibiting tunneling splittings, the value for the torsional energy splitting was held fixed to its value for the normal species. Results of these fits and line transitions may be found in the Supporting Information (Tables S7−S18).

The inertial data from the ^{13}C species were used to derive the carbon-backbone structure for the most stable conformer of propofol. Assuming that no large amplitude motions are present except for the OH internal rotation coordinate, substitution and effective structures[27,30] were derived for the rigid carbon skeleton. The experimental and ab initio structural parameters may be found in the Supporting Information (Tables S19−S20). In Figure 5, the substitution structure is graphically compared to the ab initio structure of conformers GG and Gg. This

(22) (a) Plusquellic, D. F.; Suenram, R. D.; Maté, B.; Jensen, J. O.; Samuels, A. C. *J. Chem. Phys.* **2001**, *115*, 3057. (b) Plusquellic, D. F. *User Guide to the JB95 Spectral Fitting Program*; National Institute of Standards and Technology: Gaithersburg, MD; http://physics.nist.gov/jb95.
(23) (a) Larsen, N. W.; Mathier, E.; Bauder, A.; Günthard, Hs. H. *J. Mol. Spectrosc.* **1973**, *47*, 183. (b) Attanasio, A.; Bauder, A.; Günthard, Hs. H. *Mol. Phys.* **1972**, *23*, 827. (c) Mathier, E.; Welti, D.; Bauder, A.; Günthard, Hs. H. *J. Mol. Spectrosc.* **1971**, *37*, 63, and references therein.
(24) (a) Larsen, N. W. *J. Mol. Struct.* **1986**, *144*, 83. (b) Motoda, T.; Onda, M.; Yamaguchi, I. *Chem. Lett.* **1986**, *15*, 57. (c) Onda, M.; Motoda, T.; Yamaguchi, I. *Bull. Chem. Soc. Jpn.* **1985**, *58*, 242.
(25) Sánchez, R.; Giuliano, B. M.; Melandri, S.; Caminati, W. *Chem. Phys. Lett.* **2006**, *425*, 6.
(26) Pickett, H. M. *J. Mol. Spectrosc.* **1991**, *148*, 371.
(27) Gordy, W.; Cook, R. L. *Microwave Molecular Spectra*; Wiley: New York, 1984.
(28) Watson, J. K. In *Vibrational Spectra and Structure*; Durig, J. R., Ed.; Elsevier: Amsterdam, 1977; Vol. 6, pp 1−89.
(29) Maté, B.; Suenram, R. D.; Lugez, C. *J. Chem. Phys.* **2000**, *113*, 192.
(30) (a) Rudolph, H. D. *Struct. Chem.* **1991**, *2*, 581. (b) Rudolph, H. D. In *Advances in Molecular Structure Research*; JAI Press: Greenwich, CT, 1995; Vol. 1, Chapter 3.

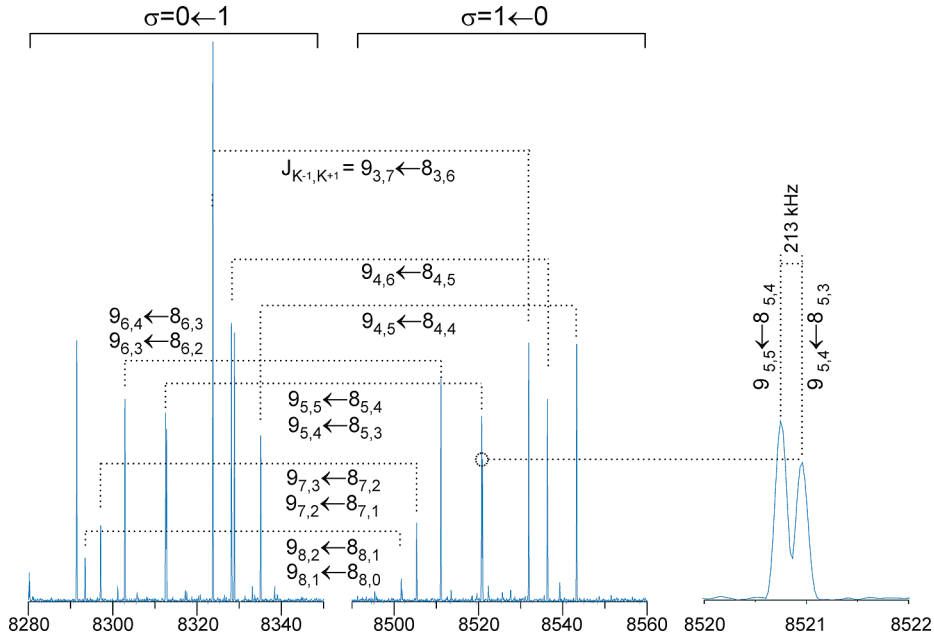

Figure 4. Two sections of 70 MHz of the microwave spectrum of propofol, illustrating the tunneling splitting in the μ_a transitions of conformer Gg due to the internal rotation of the hydroxyl group.

Table 2. Experimental Rotational Parameters for the Gg Conformer of Propofol (Tunneling Torsional Substates Labeled as $\sigma = 0$ and 1)

	fit 1[e]		fit 2[e]
parameter[a]	$v = 0$, $\sigma = 0$	$v = 0$, $\sigma = 1$	$v = 0$, $\sigma = 0/1$
A/MHz	1464.16293(41)	1464.16321(41)	1464.16304(53)
B/MHz	510.42888(16)	510.42855(16)	510.42868(20)
C/MHz	420.31238(14)	420.31229(14)	420.31234(18)
P_{cc}/u Å^2	66.44170(40)[f]	66.44186(40)	66.44182(51)
Δ_J/kHz	0.01093(33)	0.01079(34)	0.01074(42)
Δ_{JK}/kHz	−0.0085(18)	−0.0072(18)	−0.0079(23)
Δ_K/kHz	0.0542(67)	0.0535(67)	0.0538(85)
δ_J/kHz	0.00293(15)	0.00305(15)	0.00293(19)
δ_K/kHz	0.047(10)	0.046(10)	0.045(13)
ΔE_{10}/MHz[b]	104.0989(52)		104.0720(13)
s/kHz[c]	19.7		25.6
N[d]	575		575

[a] For parameter definitions, see Table 1. [b] Energy difference between the torsional tunneling substates $\sigma = 1$ and 0. [c] Root-mean-square deviation of the fit. [d] Number of transitions. [e] Standard error in parentheses in units of the last digit. [f] Conversion factor: $I_\alpha \times B_\alpha = 505379.1$ MHz u Å^2.

comparison and that of Table S19 unequivocally establish that the assigned conformer is propofol Gg, with the isopropyl α-hydrogens on the same side of the phenyl ring.

Molecular symmetry arguments corroborate this assignment. Conformers GG and Gg would both be expected to have μ_a tunneling splittings because of their equivalent isopropyl groups, but the symmetry of the two conformers is different. In conformer GG the two isopropyl groups are interchanged by a C_2 operation, while in conformer Gg they are symmetric with respect to the bc inertial plane. The two symmetries affect differently the torsion−rotation selection rules, as observed by comparison with phenol. The MS group[31] of phenol is G_4 (Table S21), and the first two torsional substates $|v = 0,\sigma = 0\rangle$ and $|v = 0,\sigma = 1\rangle$ can be ascribed to symmetries A_1 and B_2.[32] Since the electric dipole moment components of phenol transform as A_1, B_2, and B_1, the torsional selection rules $\langle\psi'_{\text{torsional}}|\mu|\psi''_{\text{torsional}}\rangle \neq 0$ require a change of symmetry $A_1 \leftrightarrow B_2$ to be connected via μ_b, the totally symmetric μ_a connects states of the same symmetry ($A_1 \leftrightarrow A_1$ or $B_2 \leftrightarrow B_2$), and transitions involving μ_c are forbidden. In propofol the selection rules depend on the relative orientation of the two isopropyl groups and can be discussed using different G_4 subgroups. Since in conformer GG the two isopropyl groups can be interchanged by a C_2 operation, the MS group would be isomorphic to the point group C_2, including only the identity (E) and permutation (P) operations of Table S21. In this case there are only two remaining irreducible representations A (μ_b) and B (μ_a and μ_c). In consequence, μ_a and μ_c must behave identically, connecting states of different symmetry ($\Delta\sigma = \pm 1$) and producing observable tunneling splittings, while the totally symmetric μ_b

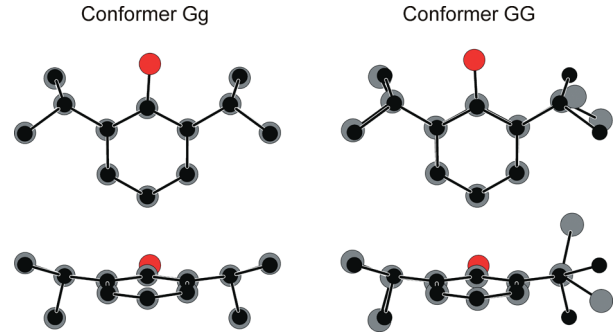

Figure 5. The assignment of the most stable conformer of propofol as conformer Gg is unequivocal from the comparison of the Kraitchman substitution structure with the ab initio geometries. In this figure the experimental carbon atom positions are in black (diameter 0.45 Å), while the calculated positions are in gray (carbon) or red (oxygen, diameter 0.65 Å).

(31) Bunker, P. R.; Jensen, P. *Molecular Symmetry and Spectroscopy*, 2nd ed.; NRC Research Press: Ottawa, Canada, 1998.

(32) Berden, G.; Meerts, W. L.; Schmitt, M.; Kleinermanns, K. *J. Chem. Phys.* **1996**, *104*, 972.

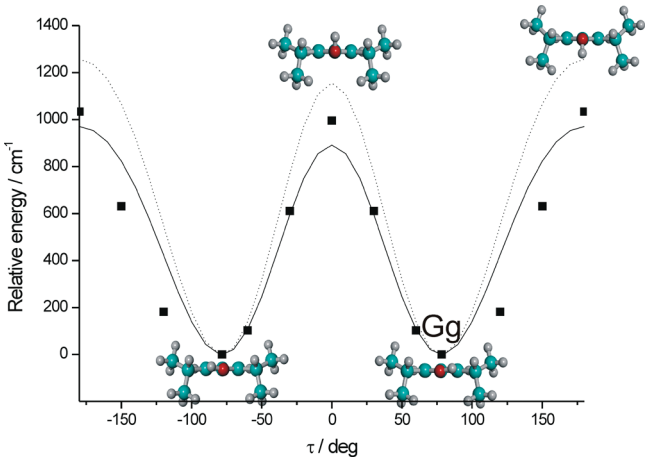

Figure 6. Potential function for the internal rotation of the hydroxyl group of propofol, as derived from the torsional splitting ΔE_{10} and Meyer's flexible model. Introduction of structural relaxation (continuous line) reduces the barrier height ($V = 905-940$ cm^{-1}) compared to the use of a rigid structure (dotted line, $V = 1172-1218$ cm^{-1}). The ab initio predictions (MP2/6-311++G(d,p), $V = 995-1035$ cm^{-1}) are represented by individual dots.

would connect torsional states of the same symmetry and these rotational transitions should be unsplit.

Conversely, in conformer Gg the two isopropyl groups can be interchanged by a reflection in the $zx = bc$ plane, so the molecular symmetry group would include the identity (E) and permutation-inversion (P^*) operations in Table S21 and would be isomorphic to C_s. Therefore, μ_b and μ_c would behave identically and totally symmetric (A′), and these rotational transitions would connect torsional substates of the same symmetry ($\Delta\sigma = 0$). On the other hand, rotational transitions involving μ_a (A″) would connect torsional states of different symmetry. In conclusion, only the μ_a transitions should produce observable tunnelling splittings, while μ_b and μ_c should be unsplit. As the observed c-type transitions of this conformer do not exhibit tunneling splittings, conformer Gg is the only conformational assignment correctly describing the torsional selection rules, consistent with the structural data.

Hydroxyl Internal Rotation Barrier of Propofol Gg. We determined the OH internal rotation barrier of the Gg conformer from the ΔE_{01} torsional splitting. Determination of 2-fold internal rotation barriers using semirigid formalisms has been discussed elsewhere.[23,24,27,33−35] For propofol Gg, we decided to adopt the monodimensional flexible model of Meyer,[36] since it allows for structural relaxation, has no symmetry restrictions, and works efficiently for few mesh points. This model has been used before for other OH internal rotation problems.[25] Initially, the hydroxyl internal rotation was modeled by ab initio methods in order to examine the structural changes associated with the OH torsion and its potential function, depicted in Figure 6. The observed global minimum Gg corresponds to a deviation from the ring planarity of 11.8° (i.e., OH torsions of $\tau = \pm 78.2$), while transition states are located for the OH perpendicular to the ring plane at $\tau = 0°$ or 180° (torsion origin on the ring side with the two isopropyl α-H). No constraints were imposed apart from the torsion angle except at the transition states where a symmetry plane was imposed to the isopropyl groups. This calculation predicts the energy at $\tau = 180°$ to be slightly higher (1035 cm^{-1} relative to the minimum) than at $\tau = 0°$ (995 cm^{-1}).

The flexible model calculations were done in three steps. We first considered a simple nonperiodic double-minimum potential function with no structural relaxation, assuming the OH motion to be prevalently on the side of the ring plane where the torsional minima are located. This model corresponds to a potential function

$$V(\tau) = B_2\left(1 - \left(\frac{\tau}{\tau_0}\right)^2\right)^2 \qquad (2)$$

where τ and τ_0 represent the torsion angle and the torsion minima relative to the transition state is defined as $\tau = 0°$. The calculated potential barrier reproducing the observed experimental torsional energy splitting was $B_2 = 1146$ cm^{-1}. More accurate values are expected using a cyclic potential function derived from the ab initio modeling:

$$V(\tau) = F(\cos\tau - \cos\tau_0)^2(1 + 0.3564\cos\tau) \qquad (3)$$

If no structural relaxation is allowed, this potential function reproduces the experimental energy difference for $F = 1346$ cm^{-1} and $\tau_0 = 78.2°$, which corresponds to torsional barriers of 1172 cm^{-1} ($\tau = 0°$) and 1218 cm^{-1} ($\tau = 180°$).

Finally, structural relaxation was introduced, allowing for changes in the reduced mass along the OH torsion path. Most of the relaxation effects are associated with the torsion of the two isopropyl groups and were modeled according to

$$\alpha(\tau) = \alpha_0 + c_1(\cos\tau - \cos\tau_0')^2 + c_2(\cos\tau - \cos\tau_0'')^2\sin\tau \qquad (4)$$

where $\alpha(\tau)$ represents the ($C_8C_7-C_2C_1$) or ($C_{11}C_{10}-C_6C_1$) torsion angles of Figure 1. The coefficients in the previous expression were calculated from the ab initio calculations as $\alpha_0 = 78.5°$, $c_1 = 3°$, $c_2 = -4°$, $\cos\tau_0' = 0.6$ and $\cos\tau_0'' = 0.92$. In this case a value of $F = 1039$ cm^{-1} was required to reproduce the experimental torsional splitting, corresponding to barrier heights of 905 cm^{-1} ($\tau = 0°$) and 940 cm^{-1} ($\tau = 180°$). In these calculations 61 mesh points were used. The main source of error in the derived barrier height is due to relaxation effects. Since the introduction of relaxation represents a change of 267 cm^{-1}, we estimate the error to be 5% of this deviation (13 cm^{-1}), assuming that most of the relaxation has been taken into account. Other model errors, like the use of approximate potential functions, increment this value, so the total error is estimated as 20 cm^{-1}.

Assignment of EG and GE Conformers. The subtraction of the transitions of conformer Gg from the full experimental spectrum in Figure 3 revealed a large number of unassigned transitions, suggesting the presence of additional rotamers. The strongest of these transitions were about 5−6 times weaker than the Gg conformer (Figure S3). While the GG conformer is the next lowest in energy, its low barrier to conformational relaxation into conformer Gg (Figure S1) depletes its population in the molecular beam, so it is not detected in the CP-FTMW spectrum. Guided by ab initio calculations of the next two conformers (EG and GE), two a-type spectra with similar rotational constants were assigned, one with an intensity approximately 10 times stronger than the other (Figure S4). Both conformers exhibited no tunneling splittings (Tables S22−S23), as expected because of the inequivalence of the isopropyl groups

(33) (a) Quade, C. R. *J. Chem. Phys.* **1967**, *47*, 1073. (b) Quade, C. R. *J. Chem. Phys.* **1968**, *48*, 5490.
(34) Bauder, A.; Mathier, E.; Meyer, R.; Ribeaud, M.; Günthard, H. H. *Mol. Phys.* **1968**, *15*, 597.
(35) Jacoby, C.; Schmitt, M. *ChemPhysChem* **2004**, *5*, 1686.
(36) Meyer, R. *J. Mol. Spectrosc.* **1979**, *76*, 266.

Table 3. Experimental Rotational Parameters for the EG and GE Conformers of Propofol

parameter[a]	conformer EG[b]	conformer GE[b]
A/MHz	1327.6876(23)	1327.6408(77)
B/MHz	540.29301(17)	537.19425(56)
C/MHz	445.44609(15)	444.28000(42)
P_{cc}/u Å^2	90.7391(11)	91.555(21)
Δ_J/kHz	0.01203(13)	0.01237(45)
Δ_{JK}/kHz	[0.]	[0.]
Δ_K/kHz	[0.]	[0.]
δ_J/kHz	0.00297(15)	0.00266(49)
δ_K/kHz	[0.]	[0.]
s/kHz	6.3	15.1
N	141	77

[a] For parameter definitions, see Table 1. [b] Standard error in parentheses in units of the last digit. Parameters in square brackets were kept fixed in the fit.

in these isomers. Fit Hamiltonian parameters for these two species are found in Table 3.

Because of the low signal levels of these two species, ^{13}C isotopologues could not be assigned in natural abundance. Therefore, other evidence must be used to make structural assignments. We noticed that the rotational parameters of the stronger species agree better with those of the EG structure, while those of the weaker species match those of the GE conformer. In particular, the P_{cc} planar moment of inertia $(=(^1/_2)(I_a + I_b - I_c) = \sum_i m_i c_i^2)$ of EG is calculated to be smaller than that of GE by 0.79 u Å^2, and likewise the stronger assigned species has a smaller P_{cc} by 0.816 u Å^2. In addition, the calculated relative energies of the EG and GE conformers ($\sim$300 cm^{-1}) suggest that the EG conformer should be more populated, as observed. Therefore, we assigned the stronger species to conformer EG and the weaker species to conformer GE. Attempts to locate the spectrum of the remaining conformer (EE) failed likely because of its low expected population ($\sim$130 cm^{-1} higher energy than GE). Moreover, the symmetric arrangement of the isopropyl groups would produce a tunneling doubling, further reducing the line intensity. The simultaneous detections of conformers EG and GE confirm our theoretical predictions suggesting relatively large barriers for conformational relaxation through internal rotation of both the isopropyl and the OH groups.

Discussion

We have fully characterized the intrinsic conformational properties of propofol using broadband chirped-pulse FT-microwave spectroscopy. Three molecular conformations were detected in the jet-cooled rotational spectrum, together with all 12 ^{13}C-monosubtituted isotopologues of the most stable conformer. The observed conformers are assigned in order of stability as Gg (global minimum), EG, and GE. The experiment thus provides information on the conformational equilibria in the isolated molecule caused by the combined internal rotation of the hydroxyl and the two adjacent isopropyl groups. Internal rotation of the isopropyl groups with respect to the benzyl ring was predicted to be hindered by relatively large barriers (e.g., 1650 cm^{-1} for interconversion between EG and the global minimum), and accordingly, conformers differing in the isopropyl orientation have been detected as independent species in the cooled expansion.

The gauche configuration of the isopropyl groups was found to be energetically favorable compared to the eclipsed orientation. This preference probably reflects the interaction between the isopropyl groups and the central hydroxyl group. No microwave investigations of isopropylbenzene have been performed, but a low-resolution electronic spectrum[37] detected only one conformer with an eclipsed α-H. This configuration is believed to reduce the steric repulsion between the methyl groups and the phenyl ring, in contrast to molecules with a single substituent at C_β, where the $C_{ipso}-C_\alpha-C_\beta$ plane is perpendicular to the ring.[29,38] Likewise, a microwave study of *p*-isopropylbenzaldehyde[39] detected two conformers corresponding to eclipsed *syn*- or *anti*-configurations of the α-H of the isopropyl group. However, there are other cases where isopropyl groups exhibit a gauche configuration. In isopropyl acetate[40] and isopropyl methyl ketone[41] (studied by gas electron diffraction) the gauche conformation was more abundant than the eclipsed conformer, as in propofol. Other isopropyl esters studied by low-resolution microwave spectroscopy also have gauche isopropyl conformations.[42] These cases have been interpreted as result of steric and electron-releasing inductive effects produced by the isopropyl group. In consequence the preferred isopropyl gauche conformation in propofol could be a result of several concurrent effects, difficult to untangle without additional experimental and theoretical data. Additional cases of steric interplay between alkyl groups have been discussed by Sandström.[43]

The hydroxyl potential energy surface of propofol Gg can also be compared to previous studies on phenolic molecules. The hydroxyl group is known to generate conformational equilibria because of its asymmetry (as in ethyl alcohol,[44] *o*-cresol,[45] or resorcinol[46]). Additionally, if the hydroxyl group is attached to a symmetric molecular frame, its internal rotation may connect equivalent minima and tunneling effects can arise in the spectrum. Internal rotation tunnelings have been previously observed in the rotational spectra of para-halogen phenols (para-X-phenol, X = F, Cl, Br),[24] para-cyanophenol[47] and para-hydroxypiridine,[25] where steric effects do not influence the potential energy barrier. The barrier heights of 905(20)−940(20) cm^{-1} determined in this work for the Gg conformer of propofol are smaller than the hydroxyl internal rotation barriers determined (Table 4) for phenol (1213(18) cm^{-1}) and those symmetric para-derivatives (1006−1513 cm^{-1}).

The magnitude of the internal rotation barrier has been related to the electron donor/acceptor capabilities of the exocyclic substituent. In the halophenols the introduction of the *p*-halogen

(37) Seeman, J. I.; Secor, H. V.; Breen, P. J.; Grassian, V. H.; Bernstein, E. R. *J. Am. Chem. Soc.* **1989**, *111*, 3140.
(38) (a) Godfrey, P. D.; Hatherley, L. D.; Brown, R. D. *J. Am. Chem. Soc.* **1995**, *117*, 8204. (b) Brown, R. D.; Godfrey, P. D. *J. Phys. Chem. A* **2000**, *104*, 5742. (c) Godfrey, P. D.; McGlone, S. J.; Brown, R. D. *J. Mol. Struct.* **2001**, *599*, 139.
(39) Bohn, R. K.; Sorenson, S. A.; True, N. S. *J. Mol. Struct.* **1992**, *268*, 97.
(40) Takeuchi, H.; Sugino, M.; Egawa, T.; Konaka, S. *J. Phys. Chem.* **1993**, *97*, 7511.
(41) Sakurai, T.; Ishiyama, M.; Yakeuchi, H.; Takeshita, K.; Fukushi, K.; Konaka, S. *J. Mol. Struct.* **1989**, *213*, 245.
(42) Silvia, C. J.; True, N. S.; Bohm, R. K. *J. Mol. Struct.* **1979**, *51*, 163.
(43) (a) Berg, U.; Sandström, J. In *Advances in Physical Organic Chemistry*; Academic Press: New York, 1989; Vol. 25, Chapter 1. (b) Berg, U.; Liljefors, T.; Roussel, C.; Sandström, J. *Acc. Chem. Res.* **1985**, *18*, 80.
(44) Pearson, J. C.; Brauer, C. S.; Drouin, B. J. *J. Mol. Spectrosc.* **2008**, *251*, 394.
(45) Welzel, A.; Hellweg, A.; Merke, I.; Stahl, W. *J. Mol. Spectrosc.* **2002**, *215*, 58.
(46) Melandri, S.; Maccaferri, G.; Caminati, W.; Favero, P. G. *Chem. Phys. Lett.* **1996**, *256*, 513.
(47) (a) Küpper, J.; Schmitt, M.; Kleinermanns, K. *Phys. Chem. Chem. Phys.* **2002**, *4*, 4634. (b) Conrad, A. R.; Barefoot, N. Z.; Tubergen, M. J. *Phys. Chem. Chem. Phys.* **2010**, *12*, 8350.

Table 4. Comparison of Internal Rotation Barriers for the Hydroxyl Group in Phenol Derivatives with Symmetric Frames

		barrier height, V/cm^{-1}	
	torsional splitting ΔE_{10}/MHz	experimental	ab initio
propofol (Gg)[a]	104.0989(52)	905−940	995−1035
phenol[b]	55.97	1213(18)	1076[f]
p-fluorophenol[c]	177.121(8)	1006(3)	
p-^{35}chlorophenol[c]	79.496(11)	1148(10)	
p-^{79}bromophenol[c]	69.73(4)	1172(10)	
p-cyanophenol[d]	20.1608(6)	1413(2)	
p-hydroxypyridine[e]	7.97(4)	1513(10)	

[a] This work. [b] Reference 23. [c] Reference 24. [d] Reference 47. [e] Reference 25. [f] Kim, K., Jordan, K. D. Chem. Phys. Lett. 1994, 218, 261.

decreases the barrier height.[24] This effect is more pronounced for *p*-fluorophenol (∼17%) but less important for *p*-chloro- or *p*-bromophenol (∼4−5%) and is attributed to changes in the double-bond character of the C−O bond. In these π-donor substituents the double bond character of the C−O bond decreases, reducing the barrier height.[24] Conversely, in 4-hydroxypyridine there is a significant increase in the barrier height (∼20%), explained as an electron-withdrawing effect of the nitrogen atom which would increase the quinonic character of the C−O bond.[25] In cyanophenol[47] the increase of the barrier height (∼14%) is smaller than in 4-hydroxypyridine. Finally, in propofol the barrier height is reduced considerably (∼25%), indicating an electron-releasing effect caused by the two isopropyl groups. This argument was previously used to justify the shortening of the C−O bond in alkyl acetates on introduction of an isopropyl group.[40] Additionally, steric hindrance effects caused by the two relatively bulky isopropyl groups are expected to influence the barrier height of propofol. The fact that the orientation of the hydroxyl group at the energy minimum is shifted from the planar configuration of phenol (5.3−11.8° for our basis sets) suggests that the steric hindrance is higher at the minimum of energy, consistent with a lower internal rotation barrier with respect to phenol. Other recent investigations of hydroxyl internal rotation have been reviewed by Caminati and Grabow.[48]

This work illustrates the advantages of chirped-pulse excitation techniques for ground-state rotational spectroscopy. The analysis of spectrally dense or multiconformer systems greatly benefits from the real multiplex advantage of chirped-pulse excitation techniques in the microwave region, which previously required extensive and time-consuming scanning with Fabry−Pérot spectrometers. Other molecular studies exploring these techniques, in particular to extend the frequency coverage to lower cm-wave frequencies and to investigate intermolecular clusters, will be presented in the near future.

Acknowledgment. Funding from NSF (Grant CHE-0618755) is gratefully acknowledged. A.L. acknowledges the Spanish MICINN for a travel grant and funding (Grant CTQ2009-14364-C02-02).

Supporting Information Available: Figures S1−S4 with expanded sections of the microwave spectrum and a monodimensional cut of the PES; Tables S1−S26 with additional ab initio data, measured rotational transitions for the three observed conformers of propofol, ^{13}C species, substitution and effective structures, and character table of the G_4 molecular symmetry group; complete listing for ref 20. This material is available free of charge via the Internet at http://pubs.acs.org.

JA104950W

(48) Caminati, W.; Grabow, J.-U. Microwave Spectroscopy: Molecular Systems. In *Frontiers of Molecular Spectroscopy*; Elsevier: Amsterdam, 2008; Chapter 15.